

Modeling of magnetic bandages for drug targeting: Button vs. Halbach arrays

Urs O. Häfeli^{a,*}, Kelly Gilmour^a, Amy Zhou^a, Stanley Lee^a, Michael E. Hayden^b

^aFaculty of Pharmaceutical Sciences, University of British Columbia, 2146 East Mall, Vancouver, BC V6T 1Z3 Canada

^bDepartment of Physics, Simon Fraser University, 8888 University Drive, Burnaby, BC V5A 1S6 Canada

Available online 13 December 2006

Abstract

Magnetic targeting of drugs to diseased tissues, such as non-healing wounds or skin tumors, is a promising clinical use of magnetic microspheres. For successful magnetic targeting, a magnet must be placed in close proximity to the target tissue. In this work the forces exerted on magnetic microspheres by different arrangements of magnets including a simple square magnet, a number of button magnet arrays, and a Halbach array were simulated and compared. Magnetic bandages utilizing a Halbach array configuration were found to yield the best trapping characteristics (large and uniform force distributions) for magnetic targeting applications close to a surface.

© 2006 Elsevier B.V. All rights reserved.

Keywords: Halbach array; Magnetic bandage; Magnetic microspheres; Skin ulcer; Modeling; Magnetic drug targeting

1. Introduction

Magnetic targeting involves the delivery and concentration of drugs bound to a magnetic carrier to a target organ or tissue using a carefully chosen interplay of magnetic forces and blood flow [1,2]. The highest probability of success is reached by injecting the magnetic carriers into the arterial vessels leading to the target region. For example, by using direct intra-arterial injection, Gallo and Hassan reached a $3.5 \times$ higher brain uptake in the magnetically targeted brain hemisphere compared to the opposite untargeted hemisphere [3]. In large animals and patients, magnetic targeting of liver tumors after injection into the hepatic artery allowed more than 90% to be retained in distinct liver areas [4]. Other investigations in rabbit tumors have also confirmed that intraarterial injections lead to much higher particle uptake in the target region compared to targeting after intravenous injection [5,6].

Magnetic carriers for in vivo magnetic targeting are generally made from magnetite particles coated with polymers or other biocompatible materials [2]. In order

to maximize the trapping efficiency, the force exerted by a magnet must exceed the thermodynamic forces generated by Brownian motion [7] and the hydrodynamic forces from blood flow [8]. Hence, large magnetic microspheres must be used in magnetic targeting. From a biophysical perspective, however, the particles should be smaller than red blood cells so as not to embolize the capillaries. Magnetic particles of around $1 \mu\text{m}$ diameter seem to represent a workable compromise between these two competing requirements.

The forces for magnetic targeting have been generally produced by strong external magnets, such as rare earth neodymium–iron–boron (NdFeB) or samarium–cobalt (SmCo) magnets [9]. Alternatively, the force can be generated using conventional or superconducting electromagnets [10–12]. A third method involves magnetizable implants that are able to produce localized regions of large attractive magnetic forces deep within the body [13–16].

We are interested in optimizing the use of permanent rare earth magnets for targeting diseases relatively near the surface of the body (within 1–2 cm). This way, skin tumors could be treated with chemotherapeutic drugs or radioactive isotopes, and non-healing wounds could be treated with growth factors. For these applications, a magnetic bandage consisting of thin and light-weight magnet arrays

*Corresponding author. Tel.: +1 604 822 7133; fax: +1 604 822 3035.

E-mail addresses: uhafeli@interchange.ubc.ca (U.O. Häfeli), mhayden@sfu.ca (M.E. Hayden).

seems appealing, as it could be worn by a patient for extended periods of time (days). The attractive force between the magnetic bandage and magnetic particles will hold the latter stationary within the capillaries. This would, for example, be useful for the slow release of drugs from the magnetic particles and would lead to prolonged treatment of the desired area. For successful therapy, it is desirable (1) to maximize the trapping efficiency for magnetic particles of a certain size and magnetic susceptibility and (2) to maximize the uniformity of the distribution of the magnetic particles throughout the target region. Reaching these aims through design of the magnetic bandage is the intent of this paper.

2. Magnetic force modeling

A three-step procedure was used to obtain an estimate of the force that would be exerted on a single microsphere placed in the vicinity of various magnetic bandages. In the first step, the magnetic field \vec{B} was calculated using the commercial finite-element modeling software package Opera-3d v10.5 (Vector Fields, Aurora, IL, USA). It was assumed that each magnet or magnet array comprising the magnetic bandage was composed of uniformly magnetized NdFeB rare earth magnets with a maximum energy product (grade) of 44 MGOe (megaGauss–oersted) and a residual magnetic induction B_r of 1.35 T. A uniform Cartesian mesh with 0.1 cm increments was used for all of the work reported here. In the second step, the calculated magnetic flux density data were extracted from the modeling software and imported into the graphing and

data analysis software package Origin v7.0 (OriginLabs, Northampton, MA, USA). Numerical partial derivatives of the flux density were then calculated using standard three-point Lagrange interpolation formulae [17]. Finally, the force \vec{F} that would be exerted on a magnetic microsphere with magnetic moment m was determined using the relationship $\vec{F} = m\nabla|\vec{B}|$ [8]. For the sake of argument, calculations were performed for 1 μm diameter microspheres consisting of 30 wt% magnetite and 70 wt% poly(lactic-co-glycolic acid) (= PLGA) with densities of 5.2 and 1.0 g/cm^3 , respectively. The magnetite was assumed to be present in the form of a uniform distribution of superparamagnetic grains 10 nm in diameter possessing a volume saturation magnetization of 484 emu/cm^3 , allowing us to model the field dependence of m using a Langevin function [8].

3. Magnet geometries

The force that would be exerted on the microsphere described above if it were placed in the vicinity of various magnet arrays was calculated for five distinct geometries. In each case the same total volume of magnetized material was used to construct the bandage. The first bandage (Fig. 1) corresponds to a single square magnet (3.75 cm on each side and 0.20 cm thick) magnetized perpendicular to the large faces. The next three bandages correspond to button arrays, each comprised of four cylindrical magnets (1.50 cm in diameter and 0.40 cm thick) arranged on the corners of a square with 2.25 cm sides. The maximum lateral extent of these arrays was chosen so that they would

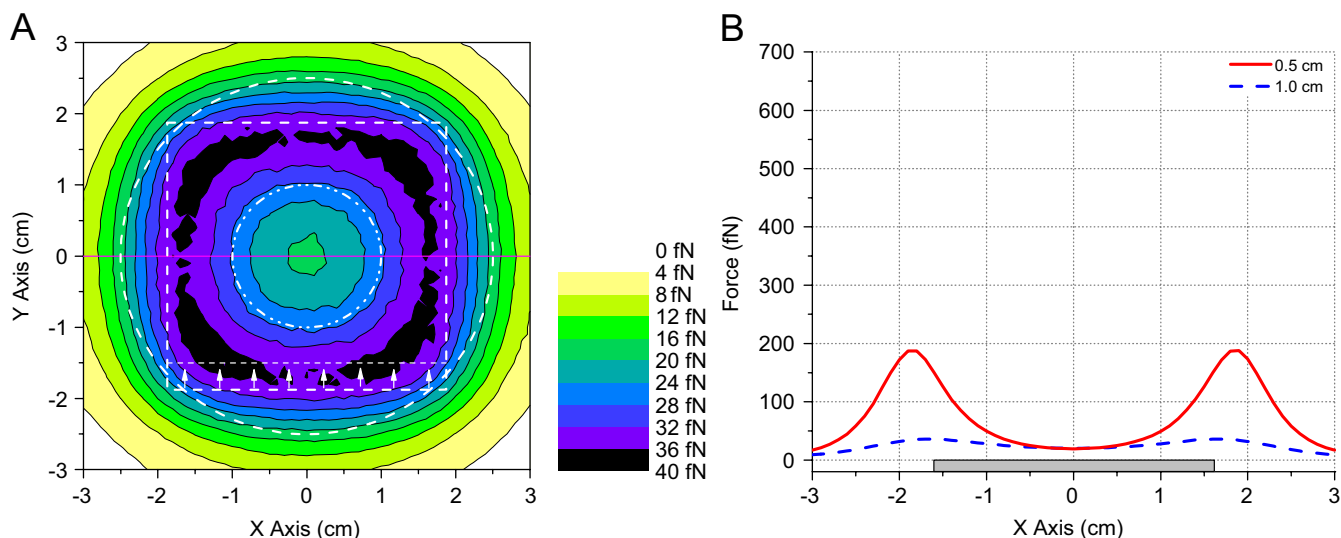


Fig. 1. Square magnet. (A) Contour plot for the magnitude of the force experienced by a single microsphere located 1 cm from the magnet surface. Here and in subsequent figures a dashed-and-dotted 2 cm diameter circle centered on the magnet (or array) is drawn to represent a loosely defined target area for the magnetic delivery of drugs. A dashed 5 cm diameter circle is also shown, and is used to demarcate a peripheral region, which one would also expect to entrap some of the magnetic particles. The white dashed outline indicates the magnet geometry, with the white arrows giving the magnetization direction. Summary statistics for the force distribution in both regions are given in Table 1 and (B) magnitude of the force at 0.5 and 1.0 cm distances from the array face. The magnet position is indicated by the gray bar.

just fit within a square 3.75 cm on each side. Again, the magnets are magnetized perpendicular to their flat faces. In the first of the button arrays (Fig. 2) all four magnets are magnetized in the same sense. In the second and third cases (Figs. 3 and 4) the orientation of two of the magnets is reversed. The array in Fig. 3 is symmetric about the x -axis and antisymmetric about the y -axis, while the array in Fig. 4 is antisymmetric about both axes. For the sake of convenience we will refer to these three arrangements as the NNNN (Fig. 2), NNSS (Fig. 3), and NSNS (Fig. 4) arrays, respectively.

The magnetic flux associated with each of the four examples described to this point exists on both sides of the array. In effect half of this flux is “wasted” in terms of magnetic trapping potential, in the sense that it does not penetrate the target region. To concentrate flux on a single side of the array, a one-sided flux structure [18,19] was selected for the fifth and final example (Fig. 5). The particular structure that we chose corresponds to one period of a symmetric eight-element Halbach array [20], constructed from rectangular bar magnets ($0.47 \times 3.75 \times 0.20$ cm) magnetized perpendicular to their long axes. The

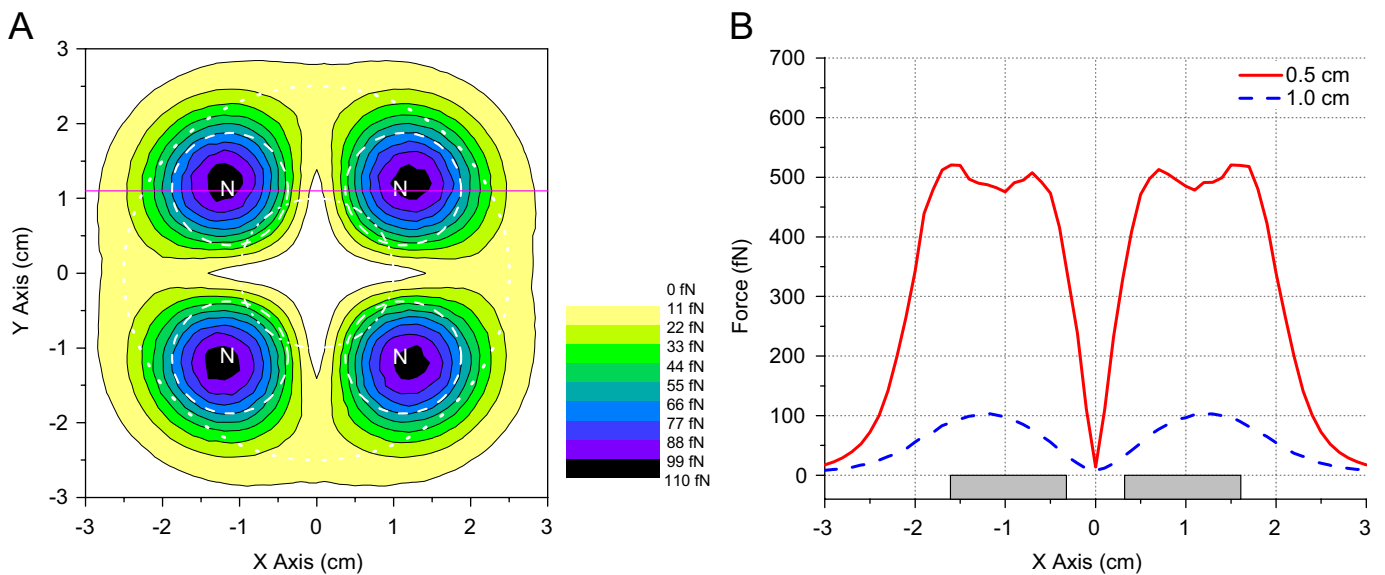


Fig. 2. NNNN button array. The magnitude of the force within the target region is low, approaching zero at the very center. (A) Contour plot for the magnitude of the force exerted on a single microsphere 1.0 cm from the surface of the array indicated by dashed circles and (B) magnitude of the force at distances of 0.5 and 1.0 cm from the array in the plane $y = 1.1$ cm which passes through the centers of two magnets.

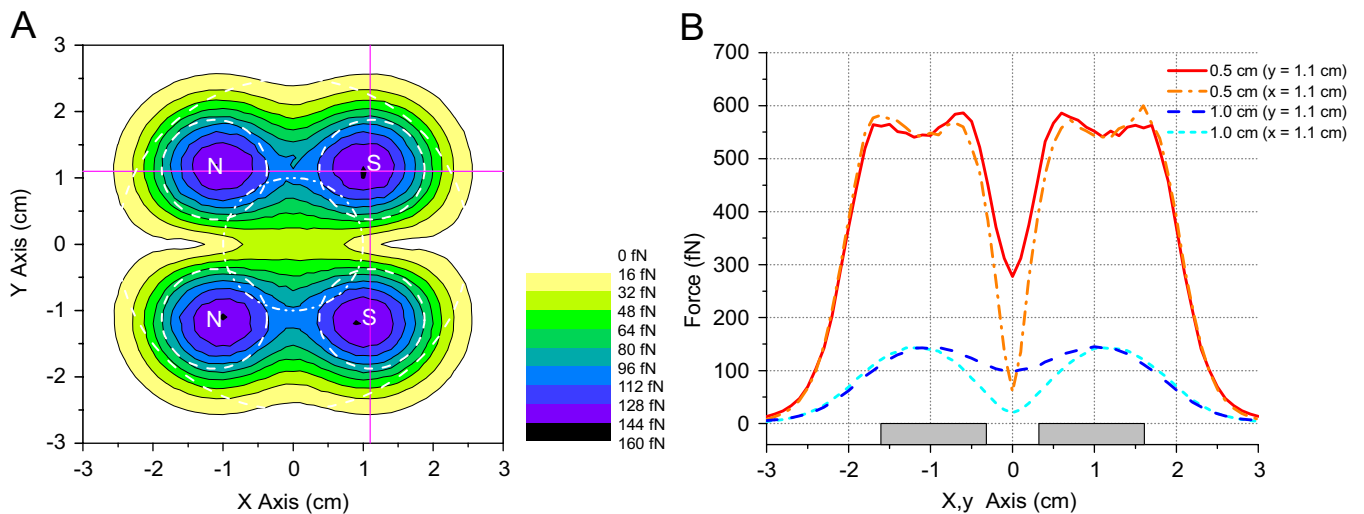


Fig. 3. NNSS button array. The mean force within the central target region is four times larger than that in the corresponding region for the NNNN array. The juxtaposition of north and south oriented magnetic dipoles produces larger field gradients. (A) Contour plot for the magnitude of the force exerted on a single microsphere 1.0 cm from the surface of the array and (B) magnitude of the force at distances of 0.5 and 1.0 cm from the array in the planes $x = 1.1$ and $y = 1.1$ cm, both of which pass through the centers of two magnets.

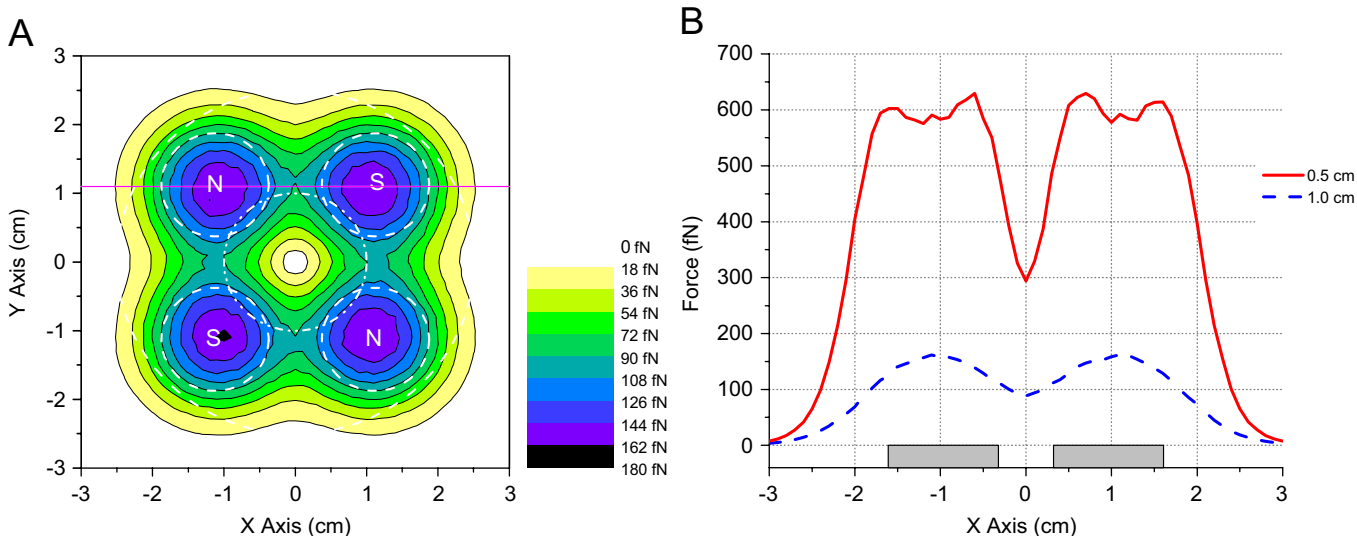


Fig. 4. NSNS button array. The mean and the maximum forces within the central target region are larger than those in previous examples. (A) Contour plot for the magnitude of the force exerted on a single microsphere 1.0 cm from the surface of the array and (B) magnitude of the force at distances of 0.5 and 1.0 cm from the array in the plane $y = 1.1$ cm which passes through the centers of two magnets.

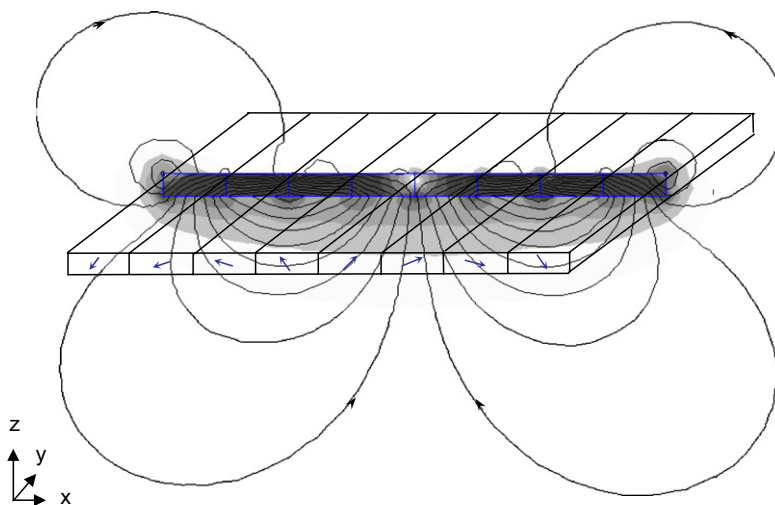


Fig. 5. Magnetic flux lines and a contour plot of the magnitude of the field gradients associated with the eight-element Halbach array described in the text is shown pictorially here as a three-dimensional projection. The dipole orientation of each element is indicated by arrows. This configuration causes most of the magnetic flux to exist below the array, which we refer to as the “strong” or “treatment” side of the array.

orientation of the magnetization vector differs by 45° between adjacent magnets. This produces the situation in which most of the magnetic flux emanates from only one of the two planar faces of the array. In addition to concentrating the magnetic flux (and thus increasing the mean force that can be exerted on a magnetic microsphere at a given distance), the Halbach array yields considerably more uniform spatial distributions of magnetic forces than simpler magnet arrays [21]. Note that once again the maximum lateral extent of this array is such that it fits within a square 3.75 cm on a side. We also note in passing that one-sided flux structures are found in applications ranging from braking systems for roller coasters and

magnetic levitation systems for trains, to the ubiquitous rubberized “refrigerator” magnet [18,19].

4. Results and discussion

Numerous and complex hydrodynamic factors influence the trapping of real magnetic microspheres. However, a simple calculation of the distribution and relative magnitude of the magnetic forces that would be exerted on a microsphere (as outlined above) provides useful insight into the relative effectiveness of magnet arrangements for drug-targeting applications. The magnet arrays described above were chosen to explore the influence of geometrical

factors on the trapping force that can be exerted on magnetic microspheres. The results are in line with expectations; as the complexity of the array is enhanced in order to increase the intensity of magnetic field gradients, the force experienced by the microspheres is increased. Fig. 1 shows the force that would be exerted on a microsphere placed in the vicinity of a single square planar magnet. The force is clearly dominated by edge effects. That is, the necessary combination of large field strength and gradient exists only around the periphery of the magnet. This force distribution represents a relatively poor scenario for medical applications, as the trapping force near the center of the magnet passes through a local minimum. Presumably, this would correspond to the middle of the targeted tissue where the need for the therapeutic drug is likely to be greatest.

Significant localized improvements in force magnitude can be made by breaking the distribution of magnetization associated with the bandage into smaller segments, as illustrated by the button array examples shown in Figs. 2 through 4. Improvements in the uniformity of the force distribution are also evident. However, all of these arrangements still give rise to regions within the treatment area where the magnetic force passes through a minimum or drops to zero. Table 1 summarizes a number of parameters that characterize the relative strength and uniformity of the forces that are potentially exerted by each of the five magnetic bandages described above. In

particular, the average value of the magnitude of the force is reported for a small central region (which is presumably the main target for therapy) and a larger surrounding region, in which microspheres will also very likely be trapped. While it is difficult to establish a simple analytic correlation between force magnitude and microsphere distribution, the presence of force minima within these regions of interest may have undesirable therapeutic consequences such as the preferential release of drugs in localized patches around the periphery of the target tissue. Further subdivision of the array into a larger number of magnets aligned solely parallel or antiparallel to one another is not generally useful. It rapidly leads to a decrease in the extent to which the field and/or field gradients (and hence the forces that are potentially exerted) penetrate the target tissue.

Careful engineering of field and field gradient distributions can yield situations in which large and uniform forces are potentially exerted over arbitrarily large surfaces. Such is the case when one-sided flux structures such as the Halbach array pictured in Fig. 5 are used [21]. It is evident from the information summarized in Figs. 6 and 7 as well as Table 1 that large forces are exerted on magnetic microspheres only when they are located on the “strong” or “treatment” side of the array. This represents a more effective use of magnetized material than that of button arrays. For example, at a distance of 1 cm the Halbach array exerts forces that are remarkably uniform in magnitude and are simultaneously significantly larger (on average more than double) than those produced near the center of the NSNS array.

Table 1
Summary statistics for force distributions in the vicinity of the five magnetic bandages

Magnet array	Center region (fN)	Surrounding region (fN)	Max (fN)	Min (fN)
<i>Distance to magnet 1.0 cm</i>				
Square	23	32	38	18
NNNN	17	51	110	1.7
NNSS	67	76	150	9.8
NSNS	76	90	160	0
Halbach strong	200	110	220	19
Halbach weak	3.8	6.8	14	0.57
<i>Distance to magnet 0.5 cm</i>				
Square	30	130	210	17
NNNN	220	320	540	14
NNSS	250	370	600	4.8
NSNS	330	400	650	0
Halbach strong	610	470	700	57
Halbach weak	37	72	190	1.7

The mean value of the magnitude of the force exerted on a single microsphere is reported for the 2 cm diameter center (or target) region (shown as dashed-and-dotted circles in Figs. 1 through 4 and 6) and the 5 cm diameter surrounding region (shown as dashed circles). Also reported are the maximum and minimum values for the magnitude of the force within the computational area. Note that statistics are provided for both sides (strong and weak) of the Halbach array.

5. Conclusions

Numerical models of magnetic flux densities and potential force distributions enable rapid and cost-effective comparisons between new magnetic bandage designs. For example, the sample calculations presented above clearly illustrate advantages of Halbach-like arrays of magnets relative to button arrays, both in terms of the strength and the homogeneity of force distributions that can be achieved. They also provide insight into pitfalls that might be encountered when more conventional magnet arrays are used. Ultimately, one would like to calculate the probability that magnetic microspheres confined to the vasculature will become trapped beneath a magnetic bandage. This is a more complex problem, requiring parameterization of blood-flow characteristics (such as velocity and viscosity), material properties (particle size distribution and magnetization characteristics), particle–particle interactions (agglomeration) and complex particle–wall interactions including extravasation. It is critical that this parameterization be accompanied by careful experimentation if realistic probabilistic trapping models are to be developed. Here again, the remarkable uniformity of the magnitude of the forces potentially exerted by Halbach arrays suggests that in many situations they may represent

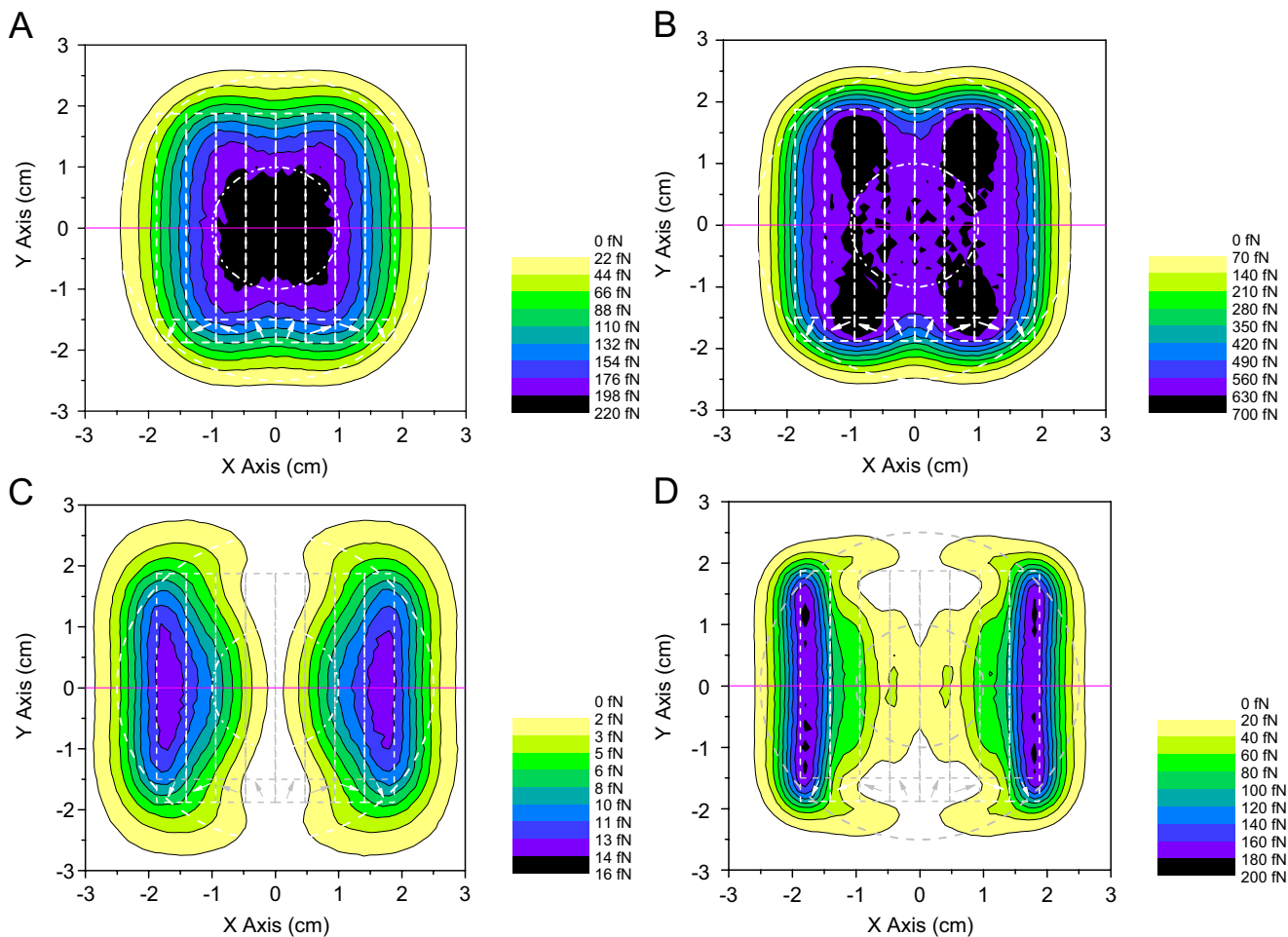


Fig. 6. Halbach array. Contour plots for the magnitude of the force exerted on a single microsphere: (A) 1.0 cm and (B) 0.5 cm from the surface of the strong side, and (C) 1 cm and (D) 0.5 cm from the weak side of the Halbach array pictured in Fig. 5. The placement of individual magnets and their magnetization are shown as dashed overlays.

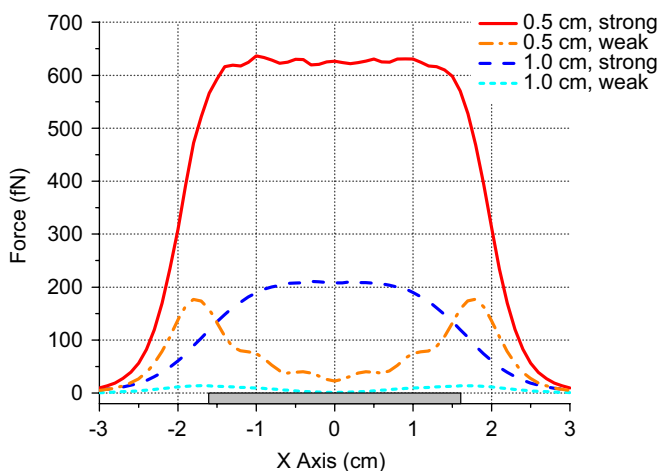


Fig. 7. Magnitude of the force exerted on a single microsphere located either 0.5 or 1.0 cm above or below the Halbach array pictured in Fig. 5, and in the plane $y = 0$ cm as indicated in Fig. 6.

an ideal geometry for both experimental and clinical applications. A magnetic bandage magnetized as a linear Halbach array is an effective geometry optimizing the

force/mass ratio, and should be pursued when the size or weight of the magnet needs to be minimized for patient comfort.

Acknowledgments

We wish to thank Peter McNeeley and Thomas Schneider for helpful discussions. We also thank the Canadian Institute of Health Research for funding support (grant number MOP-74597).

References

- [1] J. Dobson, *Nanomedicine* 1 (2006) 31.
- [2] U.O. Häfeli, in: R. Arshady, K. Kono (Eds.), *Smart Nanoparticles in Nanomedicine—the MML series*, vol. 8, Kentus Books, London, UK, 2006, p. 77.
- [3] E.E. Hassan, J.M. Gallo, *J. Drug Target* 1 (1993) 7.
- [4] S. Goodwin, C. Peterson, C. Hoh, et al., *J. Magn. Magn. Mater.* 194 (1999) 132.
- [5] C. Alexiou, W. Arnold, R.J. Klein, et al., *Cancer Res.* 60 (2000) 6641.

- [6] C. Alexiou, R. Jurgons, R.J. Schmid, et al., *J. Drug Target* 11 (2003) 139.
- [7] A. Hoffmann, S.H. Chung, S.D. Bader, et al., in: V. Labhasetwar, D.L. Leslie-Pelecky (Eds.), *Biomedical Applications of Nanotechnology*, Wiley, 2005, p. 1.
- [8] C.F. Driscoll, R.M. Morris, A.E. Senyei, et al., *Microvasc. Res.* 27 (1984) 353.
- [9] D. Goll, H. Kronmüller, *Naturwissenschaften* 87 (2000) 423.
- [10] M.S. Grady, M.A. Howard, R.G. Dacey, et al., *J. Neurosurg.* 93 (2000) 282.
- [11] G.T. Gillies, R.C. Ritter, W.C. Broaddus, et al., *Rev. Sci. Instrum.* 65 (1994) 533.
- [12] S. Takeda, F. Mishima, S. Fujimoto, et al., *J. Magn. Magn. Mater.*, (2006) this issue.
- [13] S.Y. Makhmudov, A.A. Kuznetsov, V.I. Filippov, in: U. Häfeli, W. Schütt, J. Teller, et al. (Eds.), *Scientific and Clinical Applications of Magnetic Carriers*, Plenum Press, New York, 1997, p. 495.
- [14] G. Iacob, O. Rotariu, N.J.C. Strachan, et al., *Biorheology* 41 (2004) 599.
- [15] H. Chen, A.D. Ebner, A.J. Rosengart, et al., *J. Magn. Magn. Mater.* 284 (2004) 181.
- [16] B.B. Yellen, Z.G. Forbes, D.S. Halverson, et al., *J. Magn. Magn. Mater.* 293 (2005) 647.
- [17] M. Abramowitz, I. Stegun, *Handbook of Mathematical Functions*, Dekker, New York, 1970.
- [18] J.C. Mallinson, *IEEE Trans. Magn.* 9 (1973) 678.
- [19] H.A. Shute, J.C. Mallinson, D.T. Wilton, et al., *IEEE Trans. Magn.* 36 (2000) 440.
- [20] K. Halbach, *J. Appl. Phys.* 57 (1985) 3605.
- [21] M.E. Hayden, U.O. Häfeli, *J. Phys. Cond. Matter* 18 (2006) S2877.